Bending Machine for Testing Reliability of Flexible Electronics

Daniel Nilsen Wright*, Astrid-Sofie B. Vardøy*, Branson D. Belle*, Maaike M. Visser Taklo*,
Olle Hagel†, Li Xie†, Magnus Danestig† and Torbjörn Eriksson†

*Smart Sensor Systems, SINTEF Digital
Forskningsveien 1, 0373 Oslo, Norway
Email: Daniel.nilsen.wright@sintef.no
†ThinFilm Electronics ASA
Westmansgatan 27, 582 16 Linköping, Sweden

Abstract— A novel bending machine has been designed and tested. It enables flexible electronics to be subjected to repeated bending with constant radius and tension. *In-situ* electrical characterization can give accurate analysis of lifetime distributions if sufficiently many samples are ran to failure, allowing reliability prediction models to be developed. Four sets of test samples with different combinations of substrate, routing, interconnect technology and components were examined. A poor level of reliability was observed when using anisotropic conductive paste to form interconnects, whereas a significantly higher level of reliability was observed when using a bismuth-tin solder paste. The assembly of larger components resulted in shortened time to failure, whereas increasing the bending radius prolonged the observed lifetimes.

Keywords—bending; flexible electroics; hybrid integration; Weibull analysis; in-situ measurement; ACP; BiSn; PET; PEN; PI

I. Introduction

Cheap, flexible electronics have potential uses in many areas where the flexibility itself is one of the defining characteristics of the product, e.g. in clothes, toys and other electronic products. Even though these electronics can be very cheap due to the large-scale roll-to-roll manufacturing process, there is still an expectation that they will function after exposure to the strains and stresses expected during bending. Having a repeatable and representative way to characterize the reliability of flexible electronic systems in relation to bending can be of high importance when developing such products.

Several techniques have been used to subject flexible electronics to bending. A simple method is the static test where the substrate is wrapped around a cylinder of a certain radius, with the possibility of probing the electronics while in the bent state [1]. This technique will not give any information about the reliability of the product in real working conditions, but merely an indication of tolerance to being subjected to a bent state. For reliability analysis, repeated bending is necessary. A common type of bending test is similar to the dynamic bending stress test in ISO/IEC 10373-1 [2] for credit cards, where the two ends of the test sample are compressed end-to-end, forcing the samples to bend. This results in a bending action where the radius decreases until it reaches a minimum. A potential problem when using this method on flexible electronics is that the rigidity of the attached components can influence the resultant bending radius in addition to the stiffness of the

material being bent [3]. A better technique is to roll the flexible electronics substrate repeatedly over a cylinder, thereby keeping the bending radius constant [1], [4].

In this work, a bending machine has been developed with the following criteria:

1. Constant bending radius, but possible to vary between experiments

2. Constant tension, but possible to vary between experiments

3. *In-situ* measurement of electrical properties to analyze the number of cycles before failure

In this work, different sample systems have been subjected to repeated bending and statistical analysis has been carried out to develop lifetime models for the systems.

II. Experimental

A. Bending Machine Design

The developed bending machine can be seen in Fig. 1. It consists of a horizontal motorised cylinder (a), whose motion is actuated by a 12 V DC motor with a 1:3240 gear ratio (b) and controlled by a digital control unit (DCU) (c). The DCU receives positional information from optical sensors (d) that can be adjusted to accommodate for different sample lengths. The test samples are clamped to the cylinder by 3D printed test probe holders (e). Constant tension is applied to the samples by fishing weights (f) that are clamped to the bottom of the samples. During bending, the electrical characteristics are logged to a Keysight 34972A data logger.

The cylinder has a radius, r, of 25 mm and a length of 300 mm, enabling simultaneous testing of six of the samples tested in this study. An add-on with $r = 60$ mm was made that could test two samples simultaneously.

As a safety measure, the unit is programmed to shut off the motor if the current exceeds 3 A (indicating a faulty motor) or if the motor has not changed direction in 30 s (indicating faulty optical detectors). With the current choice of motor and gear, the maximum continuous torque the system can tolerate is 2.4 Nm. This corresponds to a maximum weight of about 9.8 kg at $r = 25$ mm and 4.1 kg at $r = 60$ mm. To reduce the load on the motor and avoid current spikes that might trigger the safety
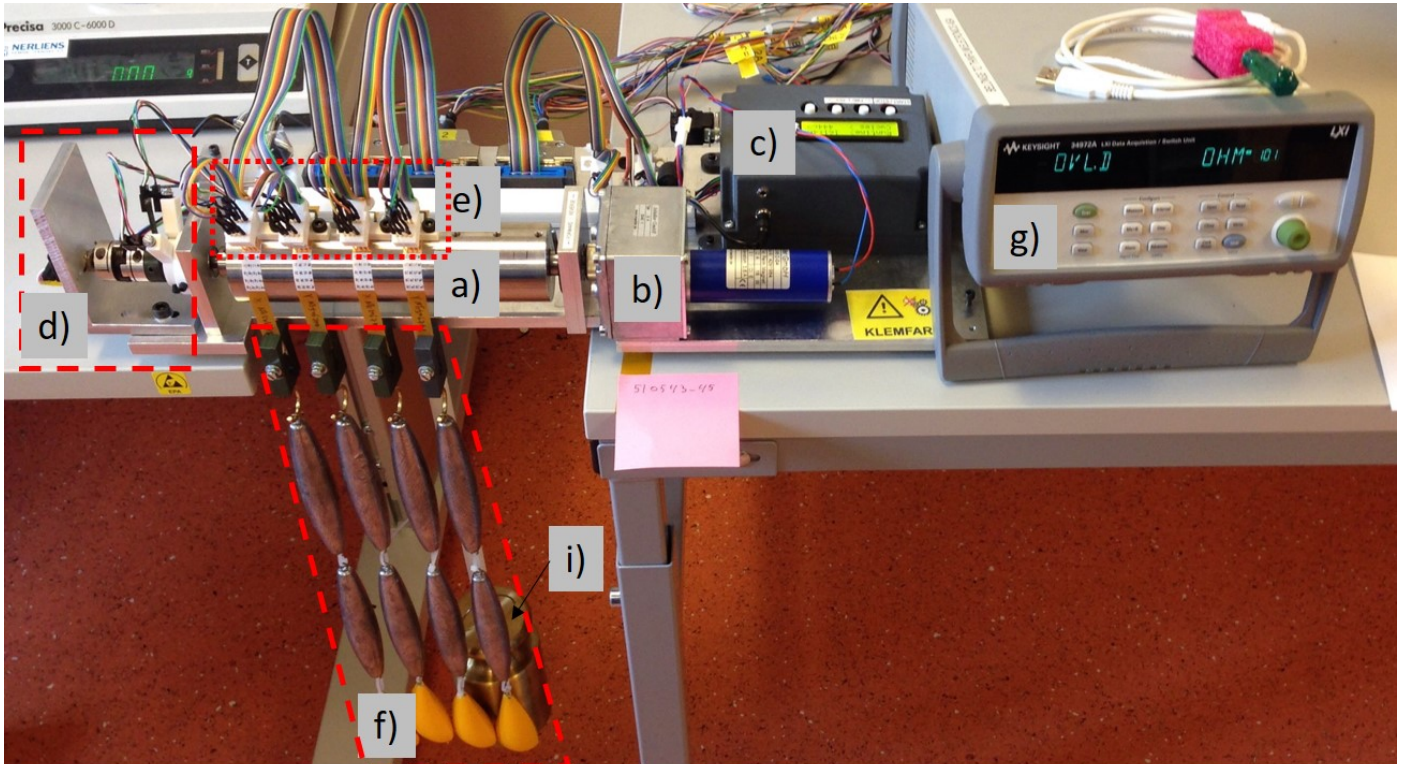
Fig. 1. The full bending machine setup. The horizontal steel cylinger, a), is actuated by a geared DC motor, b), controlled by a digital control unit, c) using signals from optical position sensor, d). Samples are clamped to the cylinder by 3D printed test probe holders, e), while constant tension is supplied by bottom clamps and fish weihgts, f). During bending, electrical properties are logged by a Keysight 34972A data logger, g). To lessen the load on the DC motor, a counterweight of 5 kg is included, i).

mechanism and stop the machine, a counter-weight of 5 kg has been applied (i). Additionally, upon changing direction, the motion is paused for 0.5 seconds, which also reduces current spikes. Based on experience, this also drastically reduces the tear on the brushes and commutator of the DC motor, prolonging the motor life.
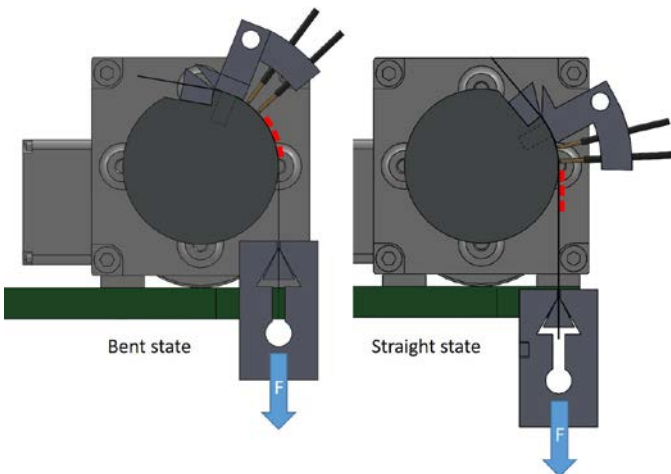
Fig.2. Cross section of the bending machine to illustrate how the samples are attached. 3D printed blocks are attached to the samples by glue or double-sided tape. Notice that the part of the sample being probed is always in a static bent state whereas the region of the sample with attached components is repeatedly bent and flattened.

B. Sample attachment

To attach a sample, 3D-printed plastic blocks are attached to both sides of the sample using either super glue or double-sided tape, depending on the expected load. The top blocks ensure sample positioning registration to make sure the measurement pads are in the correct locations for the test pins. The underlying block rests in a 5 mm deep notch in the cylinder, as seen Fig. 2, holding the sample in place before the clamp is placed. Each clamp holds two samples and contains two sets of eight measurement test probes to enable *in-situ* measurements.

C. Sample Design and Composition

The samples designed for this work consisted of rigid components attached on a flexible substrate. Two different sample designs were implemented as illustrated in Fig. 3. Both designs had four measurement pads enabling *in-situ* 4-wire resistance measurements during the bending operation. The first design, WD-R, was designed with two daisy chains consisting of five 0402-type 0-Ω resistors on each chain, oriented with the long side perpendicular to the bending axis. The second design, WD-I, had an additional 3 mm x 3 mm, 16-pin integrated circuit (IC). The IC was programmed to operate as nine parallel resistors on pins 1,2 and 4-10. The resistance measured between pads A and D was approximately $28/n$ Ω, where n signifies the number of pins electrically connected to the substrate. In theory therefore, one could analyze how many of the pins that had lost electrical contact to the substrate. The

IC had to be powered with a 5 V power supply during bending to measure the resistance.

Four groups of samples were tested in this study. They had one of three different material combinations:

a) Anisotropic conductive paste (ACP) on screen printed silver (Ag) pads on polyethylene naphthalate (PEN) substrate

b) Bismuth-tin (BiSn) solder on laminated copper (Cu) pads on polyethylene terephthalate (PET) substrate

c) BiSn solder on laminated Cu on polyimide (PI) substrate.

The assemblies are summarized in Table I. Details of the manufacturing process can be found in [4].

TABLE I.   SUMMARY OF THE SAMPLES TESTED IN THIS WORK

Group	Component	Interconnect	Pad material	Substrate	Substrate thickness (μm)
G1	0402	ACP	Ag	PEN	100
G2	0402	BiSn	Cu	PET	125
G3	0402	BiSn	Cu	PI	50
G4	IC	BiSn	Cu	PI	50

D. Design of Experiment

In order to establish the relevant tension range for the repeated bending tests, static tension tests were performed. At least two of each sample type were placed in the bending machine in the bent state. The tension was incrementally increased by sequentially adding weight to the bottom clamp and subsequently reading the resistance. It was assumed that the friction between the sample and the steel cylinder was not significant enough to affect the tension seen by the sample. The
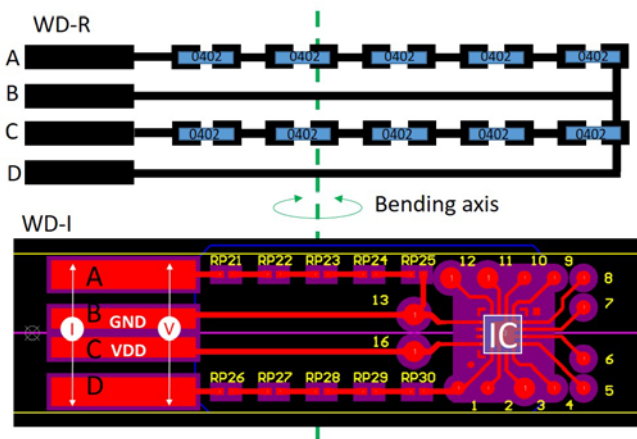
Fig. 3. Illustrations of the two samples used in this study. Top: WD-R sample with double daisy chain with five 0402 0-Ω resistors in each chain. Bottom: WD-I designed for a 3 mm x 3 mm IC with 16 pins.

failure condition for all tests in this study was an increase in resistance of 20% above the initial value. The value at which the failure condition was reached, defined the failure tension, T_{fail}, of the sample type.

For the repeated bending cycle tests, the tension used was stated as a percentage of T_{fail}, in order to compare samples with different material combinations to some extent.

WD-R samples were only bent using the r = 25 mm cylinder, whereas the WD-I samples were also tested using the $r = 60$ mm setting.

Experiments were typically run until all samples showed failure. In a few exceptions, the test time became unacceptably long and the experiments were stopped earlier.

E. Data Analysis

The DCU was programmed to output a voltage of -3.5 V when the samples were in the straight state and +3.5 V when the samples were in the bent state. This data was used to define which cycle each data point belonged to. The number of data points per cycle depended on the length of the cycle and the number of samples being measured. The logged data could then be analyzed with respect to cycle number.

The most relevant state for application was assumed to be the straight state and based on initial experiments made on samples using ACP on Ag lines, this was also the state at which the resistance was at a minimum during each cycle. Hence, the minimum resistance at each cycle was analyzed and used as the figure of merit. For each sample type and applied tension, the cycle at which the resistance reached the 20% increase threshold was summarized and fitted to the cumulative Weibull distribution function,

$$F(x) = 1 - exp(-\lambda x)^k \qquad (1)$$

where λ is the scale parameter and k is the shape parameter. The scale parameter signifies at which cycle 63.2% of the samples have failed. The shape parameter has three different ranges of significance [4]. If $k < 1$, the number of failures decreases with the number of bending cycles and is often attributed to manufacturing or assembly problems of the product. If $k = 1$, the rate of failures is constant and is typically attributed random failures. If $k > 1$, the failure rate is increasing with time, due to gradual degradation of the product.

III. RESULTS AND DISCUSSION

A. Tension tests to establish T_{fail}

In Fig.4 the relative resistance, $R(T)/R(T=0)$ is plotted against applied tension, T, for all sample groups. All groups were tested at $r = 25$ mm, while G4 was also tested at $r = 60$ mm.

In contrast to the other groups, group G1 had a nearly instant and steady increase in $R(T)$. As G1 was the only group with ACP interconnects, one can conclude that the increasing $R(T)$ is due to changes in the ACP, most likely a gradual decrease in contact area between the conductive particles in the ACP and the two conductive surfaces [5]. The gradual increase leads to failure at 32 ± 3 N/mm^2.
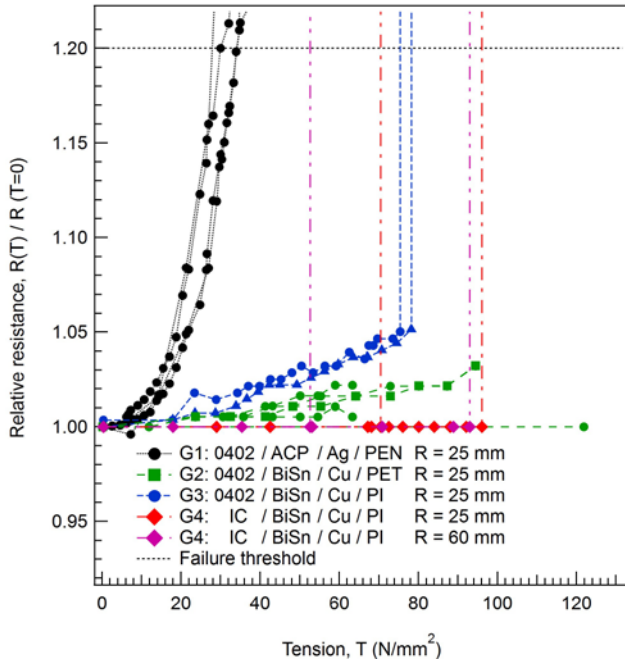
Fig. 4. The relative resistance plotted against the applied tension for establishing the tension at failure, T_{fail}, of the different sample types.

In contrast, group G2 did not fail, even at $T = 121$ N/mm^2, where the experiment was stopped for practical reasons. This suggests that a combination of PET substrate with BiSn interconnects on Cu pads is a robust flexible electronics system with respect to bending. The maximum increase in $R(T)$ was only 3% at $T = 94$ N/mm^2. T_{fail} for G2 was set at 121 N/mm^2.

Group G3 showed a steady but slow increase in $R(T)$ from $T = 20$ N/mm^2 to $T = 75$ N/mm^2, at which point the resistance increased suddenly to ∞ in a few seconds. This behavior suggests that electrical contact was lost due to micro-cracks in the conductive copper lines caused by the substrate stretching. In fact, when the tension was released, $R(T)$ returned to normal values.

Groups G4 and G5 had no increase in $R(T)$ until failure. One reason for this was higher initial values so that any small increases in $R(T)$, as seen for G2 and G3, were not measurable in the ranges used. The other reason was that the first pins to lose electrical connection to the substrate was either of the pins needed to supply 5V to the IC (pins 13 and 16), as seen in Fig 5. If any of pins 1, 2 or 4-10 had lost connection, one would recognize this as a step-wise increase in R, as stated in section II C. It is somewhat surprising that one of the samples in G5, measured at $r = 60$ mm, had a lower T_{fail} than G4, measured at $r = 25$ mm. However, the number of samples for the tension tests were limited and not sufficient for a comprehensive statistical analysis of that particular phenomenon.

TABLE II. SUMMARY OF T_{FAIL} FOR THE FIVE SAMPLES GROUPS

	G1	G2	G3	G4	G5
T_{fail} (N/mm^2)	32 ± 3	121*	81 ± 1	85 ± 21	93 ± 6
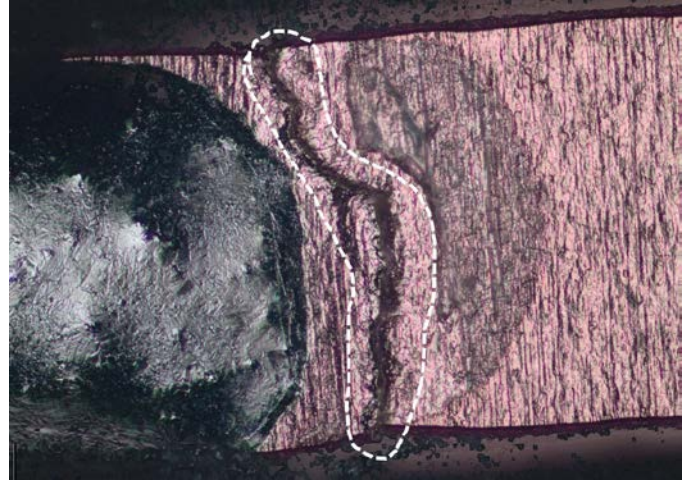
Fig. 5. A crack in the Cu track at the edge of the BiSn fillet for pin 16 on the IC.

* Highest value tested (did not fail).

B. Repeated bending

Five samples from group G1 were bent with a tension 33% of T_{fail}. As seen in Fig 6, the resistance is shown to steadily increase with number of cycles. The first failures were reached at about 1000 cycles while the last sample fails at about 4000 cycles. It is clear from Fig. 6 that the increase in R solely comes from the ACP interconnects (black curves), since the printed Ag lines (blue curves) were shown not to be affected by the repeated bending in the range of cycles applied in our study. This is in contrast to Happonen et al. [6] who estimated, using a Coffin-Manson curve fit, that Ag lines bent at a 25 mm radius in tensile
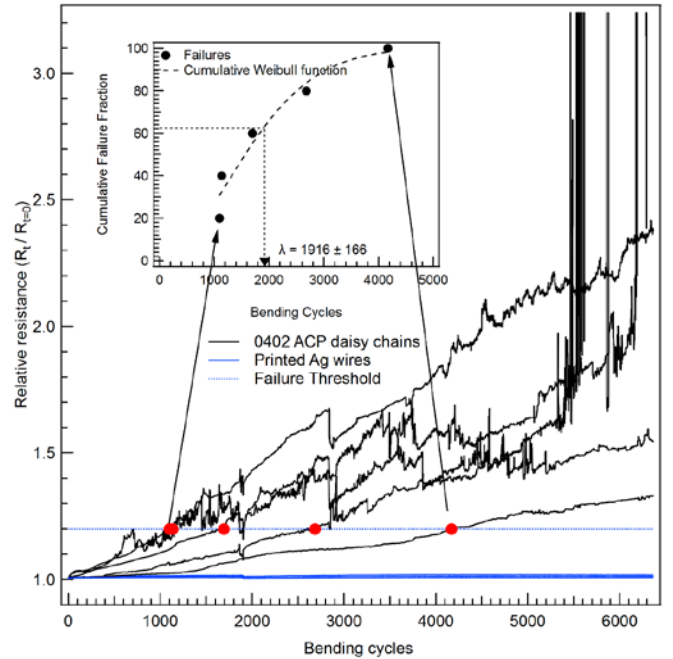
Fig. 6. Evolution of the relative resistance versus bending cycles for sample group G1. The repeated bending causes the ACP to fail before 5000
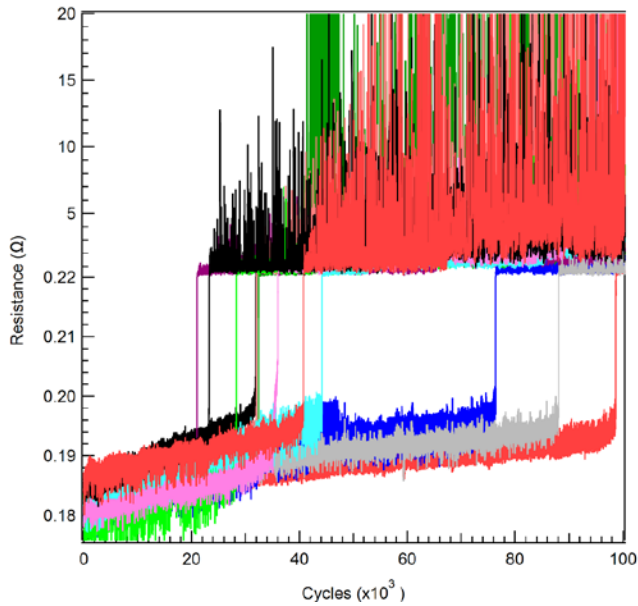
Fig. 7. Minimum cycle resistance versus bending cycle for group G2 with BiSn / Cu / PET. All samples show first a gradual increase in R up to 10%, after which R oscillates at a level 2-3 orders of magnitude higher than the original resistance.
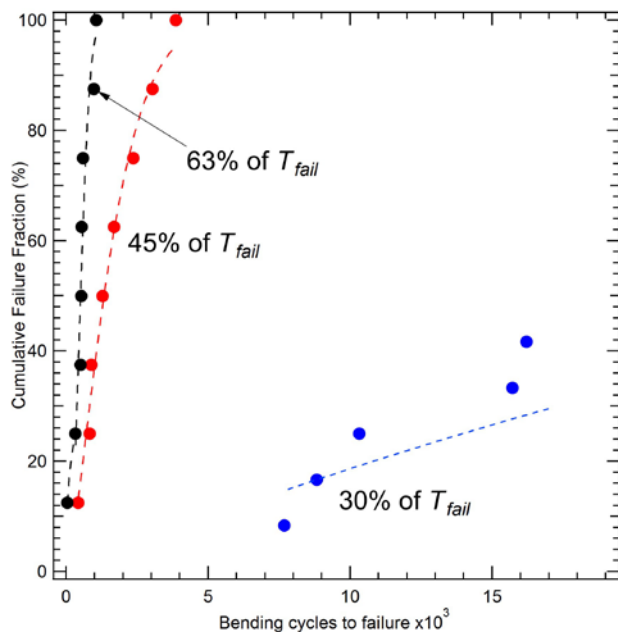
Fig. 8. Failure data for group G3 bent with tensions of 30%, 45% and 63% of T_{fail}. The Weibull fit for the 30% case is highly influenced by "right censored" data, i.e, samples that were not bent until they failed.

mode should fail just before 5000 cycles. However, Happonen

et al. did not state the tension experienced by their samples during bending.

For clarity, the inset in Fig. 6 shows the methodology for using cycle number at failure to estimate the scale parameter, λ, for a set of experimental conditions. Values for λ are summarized at the end of the article.

Six samples from group G2 were bent for a total of 130 000 times using the same weight as for group G1 (1.3 kg per sample), which constituted about 10% of T_{fail}. The behavior during cycling was distinctly different from G1. As seen in Fig. 7, all samples in G2 show an initial increase in the resistance of about 10%. At this point, the resistance increases suddenly by several ohms, after which the values oscillate between 1 Ω and 20 Ω. The mechanisms behind the behavior is currently not fully understood. One could speculate that the first increase is due to work hardening of the laminated copper tracks [7] whilst the sudden jump in resistance, is more likely caused by failure of the solder.

Group G3 was bent at 30%, 45% and 63% of T_{fail}. At 30%, the minimum cycle resistance did not show the same behavior as for group G2. Rather, a fairly constant resistance of about 300 mΩ was measured during a few hundred cycles before the resistance suddenly increased to 1 – 3 Ω, corresponding to a failure. In the bent state, the resistance oscillated between a few ohms and an open circuit. The fact that R did not increase before failure, suggests that the Cu tracks on the PI substrates did not experience the same work hardening as the Cu tracks on the PET. The Cu on the PET will experience about 2.5 x the strain, ε, as the Cu on the PI due to different substrate thicknesses. This can be estimated from the following expression from [8] ,

$$\varepsilon = (d_f + d_s) / 2r \qquad (2)$$

where d_f and d_s are the film and substrate thicknesses, respectively and r is the bending radius. Only five of the 11 samples receiving tension at 30% of Tf_{ail} were bent until failure, leaving six samples as "right censored", meaning one knows that they survived the number of bending cycles they were exposed to, but not when they would have failed. This leads to about 50% uncertainty in λ.

The samples receiving a tension of 45% and 60% of T_{fail} all showed abrupt failures at significantly lower number of bending cycles, as can be seen in Fig. 8. In Fig 9 one can see cross sections of the BiSn fillet on the Cu pad for resistors that had failed during bending. For $T = 30\%$ of T_{fail}, the main failure mode was delamination between the BiSn solder and the Cu pad. For $T = 45\%$ and 63% of T_{fail}, the main failure mode was

Fig. 9. Cross section of failed BiSn interconnects. With $T = 30\%$ of T_{fail}, the main failure mode was delamination of the BiSn from the Cu tracks. Fot $T = 45\%$ and 63% of Tfail, the main failure mode was a crack in the Cu tracks.
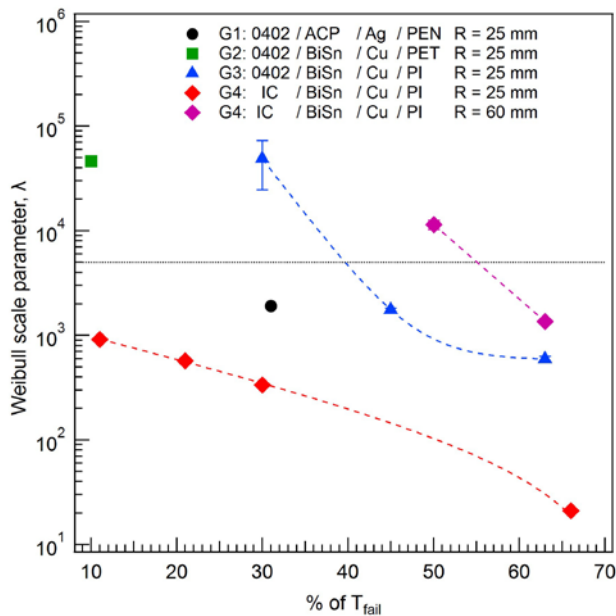
Fig. 10. Summary of the λ value for all tests done in this work, versus the percentage of T_{fail}. The specified threshold of 5000 cycles is indicated.

cracks in the Cu pad right at the edge of the BiSn fillet.

Sample group G4 had the WD-I design in which the resistance or nine parallel resistors was measured during bending. In theory, therefore, one should be able to analyze the number of interconnects that were functioning based on the measured resistance value. In practice, however, this proved to be challenging due to noisy data. It was therefore decided to continue with the same failure condition as for the other groups.

Sample group G4, was tested with T of 11%, 21%, 31% and 66% of T_{fail} using bending radius of 25 mm, and with T of 53% and 63% of T_{fail} with the larger radius of 60 mm. All samples behaved similarly to group G3 for both radii in that the measured resistance was stable until it suddenly increased to open circuit. At $r = 25$ mm, the value of λ was below 1000 cycles for all applied tensions. As can be seen in Fig. 10, which is a summary of all λ values reported in this work, the samples tolerated significantly more bending cycles when the bending radius was increased to 60 mm. For T of 53% T_{fail} a value for λ higher than the specified threshold was achieved. Any industrial standard for bending of flexible electronics are specific to the application, like the ISO/IEC 10373-1 standard

for credit cards. As the industry matures and new applications are found for flexible products with hybrid integration, such standards will be developed based on industry needs and experience. The specifications set in this work may seem arbitrary, but had a specific application in mind. Based on the results from G4, one would expect that most of the other sample groups would pass the 5000 bending cycle threshold if bent at $r = 60$ mm.

IV. CONCLUSION

A machine and method for assessing the reliability of flexible electronics with respect to repeated bending were developed. In-situ electrical characterization during repeated bending enables accurate detection of lifetime distributions which are essential for developing reliability prediction models for new products. Therefore, a selection of interconnect technology for flexible electronics, and identification of a safe range for acceptable bending during application, could be made using the machine and the methodology based on statistical methods.

REFERENCES

[1] H. U. Li and T. N. Jackson, "Flexibility Testing Strategies and Apparatus for Flexible Electronics," *IEEE Trans. Electron Devices*, vol. 63, no. 5, pp. 1934–1939, May 2016.

[2] "Identification cards:Test methods:Part 1: General characteristics," *ISOIEC Stand. 10373-1 2006-*.

[3] L. D. Landau & E.M. Lifshitz, *Theory of Elasticity*. Pergamon Press, 1970.

[4] X. Jiang, K. Kim, S. Zhang, J. Johnson, and G. Salazar, "High-Temperature Piezoelectric Sensing," *Sensors*, vol. 14, no. 1, pp. 144–169, Dec. 2013.

[5] M. M. Visser Taklo *et al.*, "Smart tags that are exactly reliable enough," in *2017 Pan Pacific Microelectronics Symposium (Pan Pacific)*, 2017, pp. 1–8.

[6] T. Happonen, T. Ritvonen, P. Korhonen, J. Häkkinen, and T. Fabritius, "Modeling the Lifetime of Printed Silver Conductors in Cyclic Bending With the Coffin #x2013;Manson Relation," *IEEE Trans. Device Mater. Reliab.*, vol. 16, no. 1, pp. 25–29, Mar. 2016.

[7] *Electronic Materials Handbook: Packaging*. ASM International, 1989.

[8] Z. Suo, E. Y. Ma, H. Gleskova, and S. Wagner, "Mechanics of rollable and foldable film-on-foil electronics," *Appl. Phys. Lett.*, vol. 74, no. 8, pp. 1177–1179, Feb. 1999.